Structural Engineering and Mechanics, Vol. 10, No. 1 (2000) 53-66
DOI: http://dx.doi.org/10.12989/sem.2000.10.1.053

Load-carrying capacities and failure modes of scaffold-shoring systems, Part I: Modeling and experiments

Y.L. Huang† and H.J. Chen†

Department of Civil Engineering, Chung-Hsing University, Taichung, 40227 Taiwan, R.O.C.

D.V. Rosowsky†

Department of Civil Engineering, Clemson University, Clemson, SC 29634-0911, U.S.A.

Y.G. Kao‡

Department of Civil Engineering, Chung-Hsing University, Taichung, 40227 Taiwan, R.O.C.

Abstract. This paper proposes a simple numerical model for use in a finite analysis (FEA) of scaffold-shoring systems. The structural model consists of a single set of multiple-story scaffolds with constraints in the out-of-plane direction at every connection joint between stories. Although this model has only two dimensions (termed the 2-D model), it is derived from the analysis of a complete scaffold-shoring system and represents the structural behavior of a complete three-dimensional system. Experimental testing of scaffolds up to three stories in height conducted in the laboratory, along with an outdoor test of a five-story scaffold system, were used to validate the 2-D model. Both failure modes and critical loads were compared. In the comparison of failure modes, the computational results agree very well with the test results. However, in the comparison of critical loads, computational results were consistently somewhat greater than test results. The decreasing trends of critical loads with number of stories in both the test and simulation results were similar. After investigations to explain the differences between the computationally and experimentally determined critical loads, it was recommended that the 2-D model be used as the numerical model in subsequent analysis. In addition, the computational critical loads were calibrated and revised in accordance with the experimental critical loads, and the revised critical loads were then used as load-carrying capacities for scaffold-shoring systems for any number of stories. Finally, a simple procedure is suggested for determining load-carrying capacities of scaffold-shoring systems of heights other than those considered in this study.

Key words: scaffolds; shores; scaffold-shoring systems; load-carrying capacities; finite element analysis; failure modes; structural analysis.

1. Introduction

The life of a structure or a building can be divided into three stages: construction, service and wear-out. The greatest potential for collapse is during the construction stage. Actually, most failures

† Associate Professor
‡ Graduate Student

which have caused casualties and the loss of large amounts of money have occurred during construction. In Europe, Matousek and Schneider (1977) surveyed 800 failure cases from insurance files. In England, Walker (1981) surveyed 120 cases, most of which occurred in Great Britain. These studies have both confirmed that failure during the construction period is much more likely than during the service period. Among all the failures that could occur in the construction stage, the most disastrous is the collapse of temporary shores (falsework). Today, wooden shores are gradually being replaced by steel shores (or scaffold-shoring systems, especially for high-clearance construction). Methods and procedures for designing and analyzing scaffold-shoring systems are essential to ensure safe performance of these temporary shoring systems. Ayyub (1989) reported that errors in construction design and procedures account for over 50% of construction failures. An economical and safe design for a scaffold-shoring system requires knowledge of its structural behavior as well as its load-carrying capacity. Recently, the load-carrying capacity of heavy-duty scaffolds has been studied using computational and/or experimental methods. Kao (1981) was the first to conduct experimental tests to study critical loads in scaffolds up to four stories. Yen *et al.* (1993-1995) studied load patterns and load-carrying capacities using full-scale tests of scaffolds up to five stories. This research was conducted jointly by Chung-Hsing University (in Taiwan, R.O.C) and Purdue University (in the U.S). Although Kao and Yen used different methods for applying loads to the scaffolds, their experimental critical loads were very similar. Later, Yen *et al.* (1997) suggested an empirical equation to determine load-carrying capacity of scaffolds not more than five stories in height. For greater numbers of stories, the empirical equation could only be validated through further experiments. In the area of computational methods, finite element analysis (FEA) has been used extensively for calculating critical loads. Researchers have modeled scaffold-shoring systems using different element types and boundary conditions. For example, Jan (1987) studied the instability behavior of scaffolds using link elements and hinged boundary conditions. Peng (1996) performed a similar analysis using beam elements and semi-fixed boundary conditions. To date, regardless of how the scaffold systems were modeled, most researchers have attempted to analyze the entire scaffold system. This required a tremendous amount of memory and CPU time.

In this study, a two-dimensional model (2-D model) was derived from an incremental analysis of a typical complete scaffold-shoring system. Since the 2-D model can predict the structural behavior of the entire system, it is recommended as a more efficient model for use in finite element analysis. Using the 2-D model, the critical loads and failure modes of a scaffold-shoring system can be computed quickly. Yen's test results (1997), along with results from additional experiments conducted for this study, were used to verify the computational model. Thus, computationally determined and experimentally validated critical loads are recommended as the load-carrying capacities for scaffold-shoring systems.

2. Establishment of the numerical model

The height of formwork is usually not simply a multiple of the height of a single scaffold. A typical scaffold-shoring system (see Fig. 1), using the definitions provided by Yen *et al.* (1997), is usually composed of two portions, posts and scaffolds. The nomenclature for each part of the scaffold-shoring system is shown in Fig. 2. The critical load for the entire shoring system can be determined by FEA, assuming all of the structural and mechanical properties can be correctly input. However, as seen in Fig. 1, there are many similar substructures that comprise the entire system.

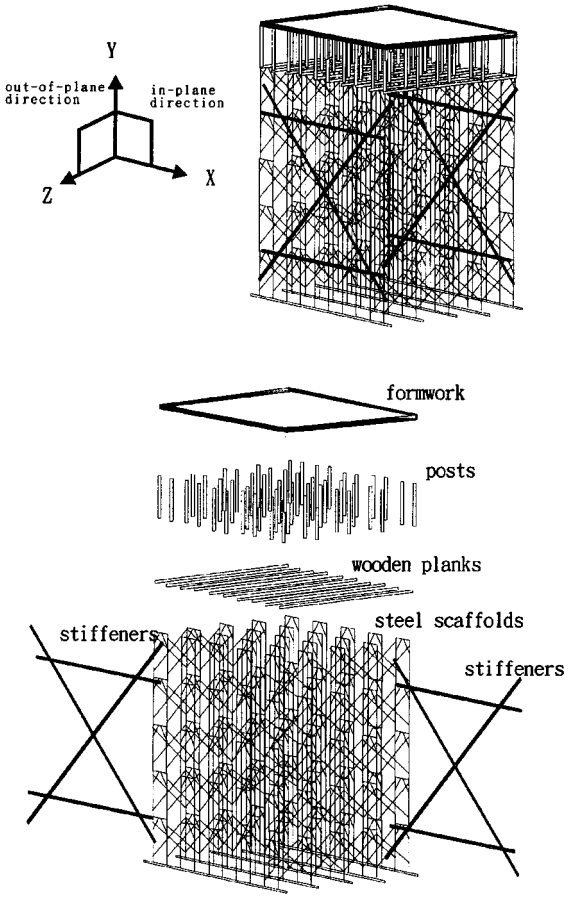

Fig. 1 Typical scaffold-shoring system (Yen *et al.* 1997)

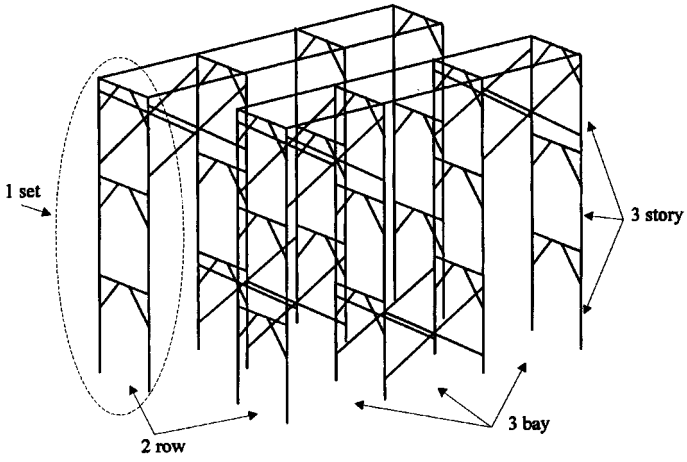

Fig. 2 Nomenclature for a scaffold-shoring system

Therefore, there should exist a simple unit structure with the same structural behavior as the entire system. One of the objectives of this study was to identify and model this simple unit. An analysis using this simplified model would offer significant computational advantages (i.e., require less time).

2.1. Assumptions

The following assumptions were made in constructing the numerical model.

(1) The connection joints of the posts and steel scaffolds are braced against sidesway as shown in Fig. 3.

(2) All scaffolds except the exterior scaffolds fail at the same time.

(3) The cross braces provide stiffness for the scaffolds against buckling in the out-of-plane direction.

(4) Both the tops and bottoms of the scaffolds are hinged.

(5) All scaffolds are made of the same linearly elastic material and are the same size.

2.2. Process to establish the numerical model

The numerical model was established through the following steps.

(1) The entire shoring system shown in Fig. 4 was modeled and analyzed using the finite element analysis software ANSYS to determine its critical load. The FEA results show that the use of lateral braces to resist sidesway at the connection joints between the posts and scaffolds has a significant effect on critical loads. For instance, the critical load for the shoring system shown in Fig. 4(a) and called Case A, without lateral braces at the connection joints between the scaffolds and posts, is 366 kN. The critical load for the shoring system shown in Fig. 5(a) and called Case B, which is the same system as Case A with additional lateral braces at the connection joints, is 1092 kN. The shoring system called Case C, shown in Fig. 6(a), which is the same as Case A but without the

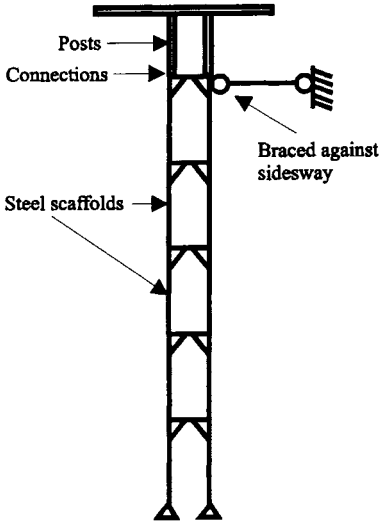

Fig. 3 Connection joints between posts and steel scaffolds braced against sidesway

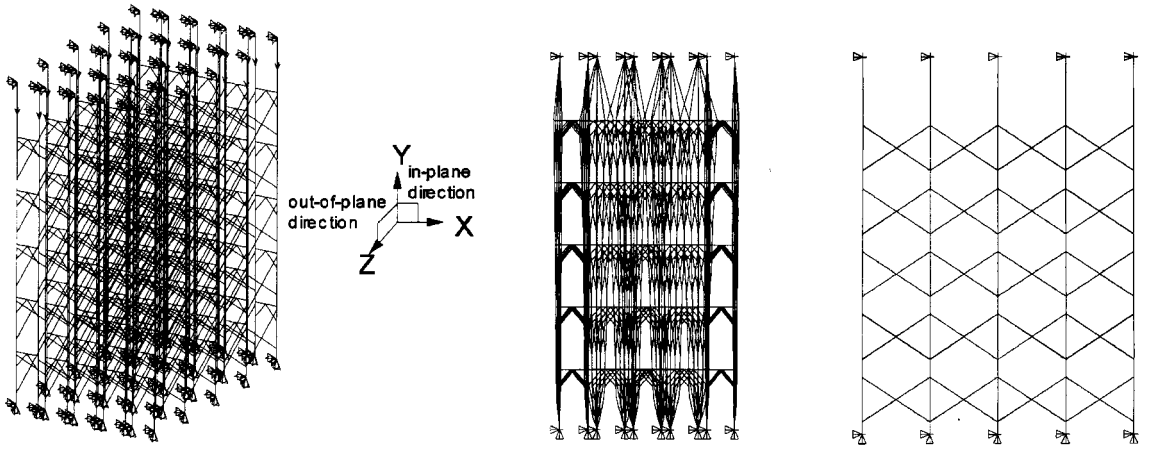

(a) Model of Case *A* (b) Failure mode in the X-Y plane (c) Failure mode in the Y-Z plane

Fig. 4 Complete scaffold-shoring model without lateral braces at connections between posts and scaffolds, Case A

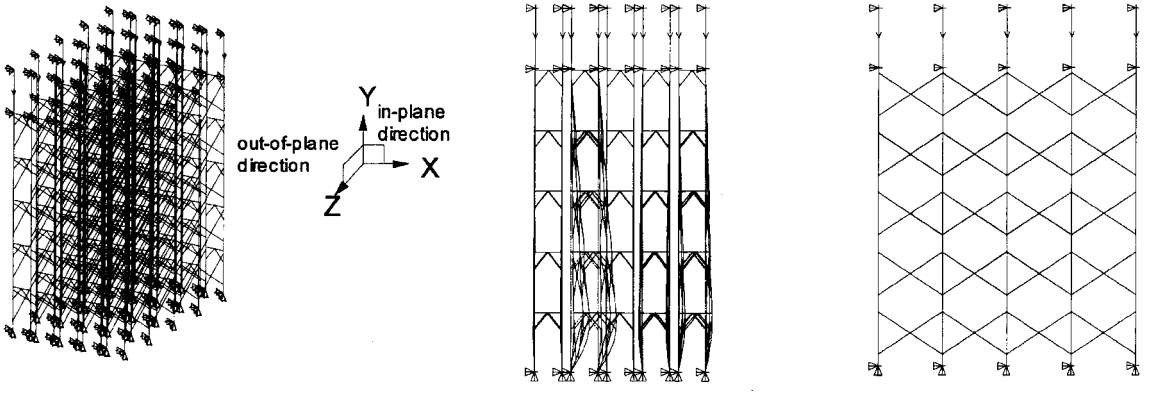

(a) Model of Case *B* (b) Failure mode in the X-Y plane (c) Failure mode in the Y-Z plane

Fig. 5 Complete scaffold-shoring model with lateral braces at connections between posts and scaffolds, Case B

posts, has the same critical load of 1092 kN. Thus, it is shown that the presence of lateral braces greatly increases critical load in systems with posts, and the critical load is exactly the same as that of the system with no posts. In addition, the relatively small critical load in Case A shows that scaffolds without braces have limited load-carrying capacity. On the other hand, from the failure modes shown in Figs. 5(b), 5(c), 6(b) and 6(c), the failure modes of Cases B and C are seen to be the same. The failure mode in all of these cases is buckling in the scaffold portion. However, the failure mode of Case A shown in Figs. 4(b) and 4(c) is different from Cases B and C. The former fails due to sidesway occurring at the connection joints between the scaffolds and posts. These computational results for failure modes and critical loads highlight the same effect of lateral braces on the shoring systems. The lateral braces are critical elements, and should be carefully installed in the field. With lateral braces, the entire scaffold-shoring system, i.e., with scaffolds and posts (Case A,

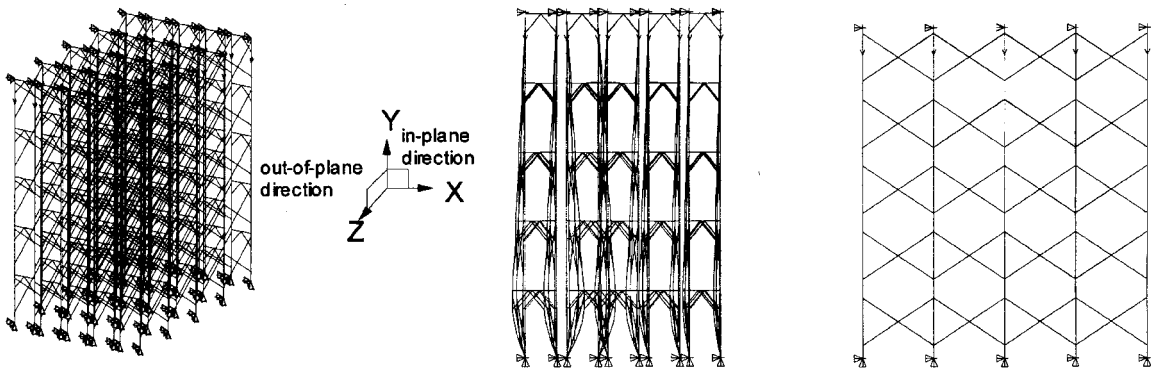

(a) Model of Case *C* (b) Failure mode in the X-Y plane (c) Failure mode in the Y-Z plane

Fig. 6 Complete scaffold-shoring model without posts, Case C

Fig. 4a), can be simplified into a system without posts (Case C, Fig. 6a).

(2) The critical load in Case C is exactly five times the critical load of the single-row, five-story scaffold system called Case D shown in Fig. 7(a). Also, the failure mode for Case D, shown in Figs. 7(b) and 7(c), is the same as that for Case C, shown in Figs. 6(b) and 6(c). Therefore, a multiple-row system can be considered a combination of single-row systems. The model for Case C is therefore simplified into a single-row model (Case D, Fig. 7).

(3) Assume that a two-dimensional model (2-D model), shown in Fig. 8(a), is composed of a one-set, five-story scaffold system and is constrained in the out-of-plane direction. Then, the critical load for Case D is exactly five times that of the 2-D model. As before, the 2-D model has the same failure mode, shown in Figs. 8(b) and 8(c), as that in Case D. Finally, the model for Case D is now simplified into a 2-D model.

Again, the 2-D model is built step-by-step from an analysis of an entire scaffold-shoring system. In its final form, the 2-D model can predict the structural behavior, including both critical loads and failure modes, of the entire system. It is therefore recommended that the 2-D model be used in

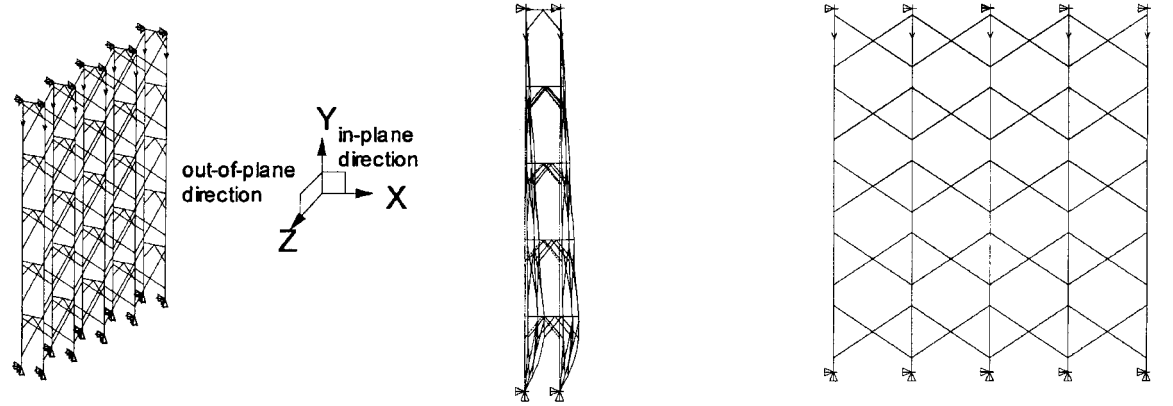

(a) Model of Case *D* (b) Failure mode in the X-Y plane (c) Failure mode in the Y-Z plane

Fig. 7 Model of one-row of scaffolds, Case D

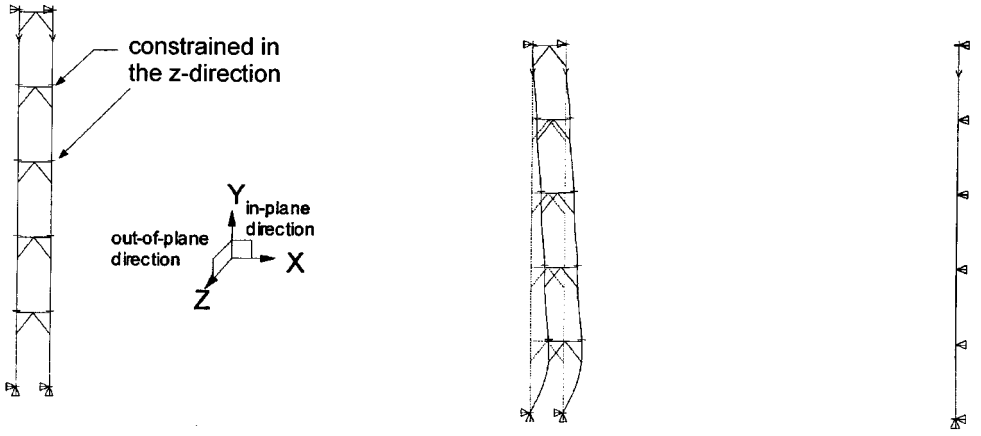

(a) 2-D model (b) Failure mode in the X-Y plane (c) Failure mode in the Y-Z plane

Fig. 8 Computational (2D) model (the 2-D model)

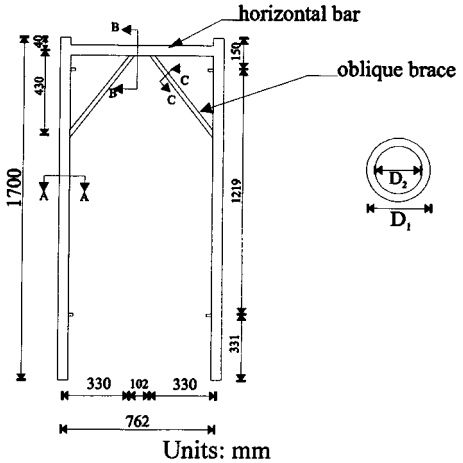

Units: mm

Section	D_1(mm)	D_2(mm)	Area(mm^2)
A	42.01	37.65	273.1
B	42.01	37.65	273.1
C	26.37	22.5	148.5

Fig. 9 Shapes and sizes of scaffold used in this study

further analytical studies of typical scaffold-shoring systems.

3. Computational results

The pattern of the scaffold used in this study is shown in Fig. 9. Its section and material properties are as follows:

section area A = 2.73 cm^2
moment of inertia I_A = 5.43 cm^4
E = 204 GPa
F_y = 515 MPa
F_u = 645 MPa

Since scaffolds are rarely used as a one-story shoring system, and the failure mode for a one-story shoring system is quite different from that of multi-story systems, the critical loads vs. number of stories relationship does not include the one-story case. The relationship between critical loads and

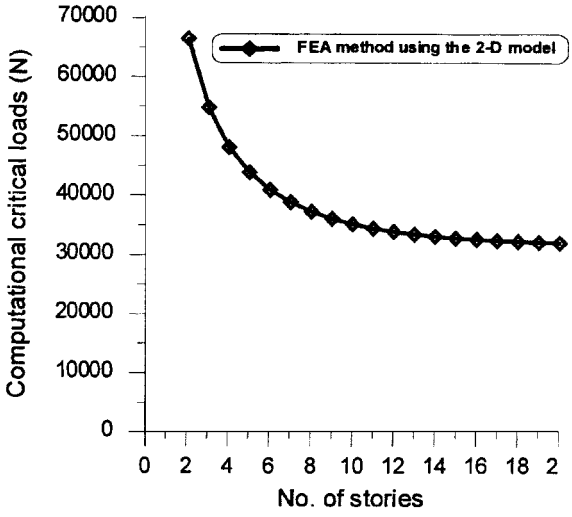

Fig. 10 Computational critical loads using 2-D model

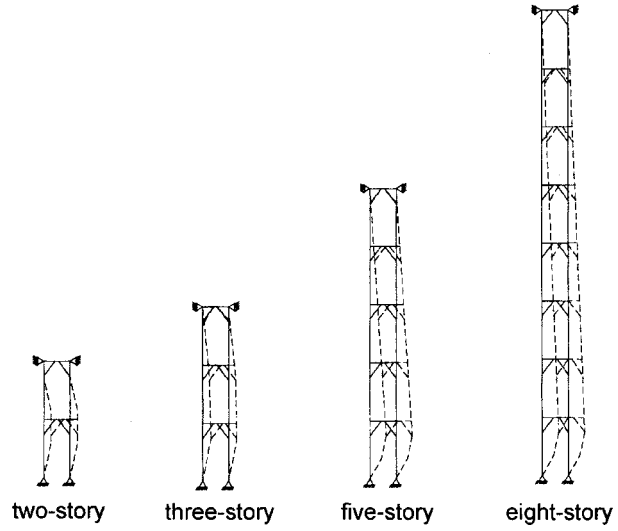

Fig. 11 Computational failure modes of 2-D model

the number of stories for the 2-D model was determined using the method described previously, and is graphed in Fig. 10. This figure indicates that computational critical load decreases as the number of stories increases. Based on the magnitudes of the critical loads, the scaffold-shoring systems are seen to fail due to buckling, since all of the critical loads are smaller than the yield load P_y= $515\times10^3\times2\times2.73\times10^{-4}$=281.2 kN. It can also be seen from the failure modes in Fig. 11 that failure of the scaffold-shoring system is due to buckling in the lowest story, and that maximum lateral displacement occurs at the top of the lowest story. The reason that buckling occurs first in the lowest floor is that the bottoms are hinge supports and there is no bottom horizontal bar. This also explains why the decrease in failure load with height does not follow Euler's rule, which states, that buckling loads (or critical loads) are inversely proportional to the square of the heights. As the scaffold-shoring system increases in height, rotational stiffness at the top of the lowest story becomes weaker, leading to a smaller critical load. Since systems always fail in the lowest story, the critical loads do not change significantly as the number of stories increases.

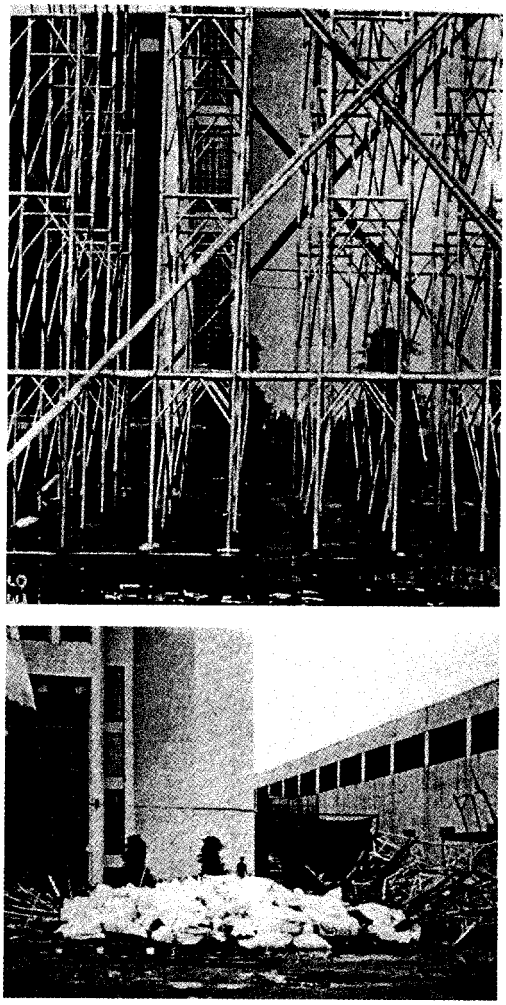

Fig. 12 Five-story full-scale test (Yen *et al.* 1997)

The computational results also indicate that the sizes of the horizontal and oblique braces shown in Fig. 9 do not significantly affect critical loads. Theory suggests that critical loads are functions of the factors of E_iI_i/L_i^2 of the vertical bars. The subscript "i" represents different-size scaffolds; L_i is the one-story height; and I_i is the moment of inertia of the vertical bars. The value of EI/L^2 for the scaffolds used in this study is $(204\times10^9\times5.43\times10^{-8})/(170^2\times10^{-4})=3830$ (N). According to the computational results in this study, the critical loads of different-size scaffolds are very close to the magnitude of the critical load in Fig. 10 multiplied by the factor $(E_iI_i/L^2)/3830$.

4. Test program and comparisons between experimental and computational results

In addition to the outdoor experimental test of five-story scaffolds shown in Fig. 12 (Yen *et al.* 1997), the following full-scale tests of scaffolds from one to three stories were performed in the laboratory.

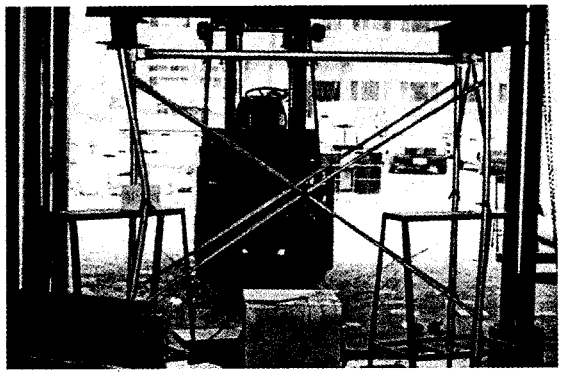

(a) Two-set, one-story tests

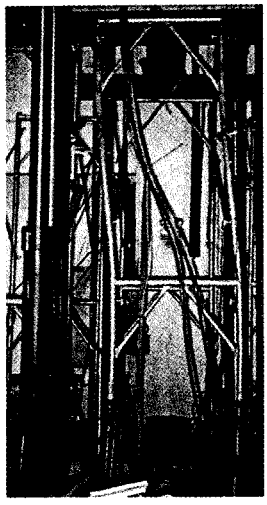

(b) Two-set, two-story tests

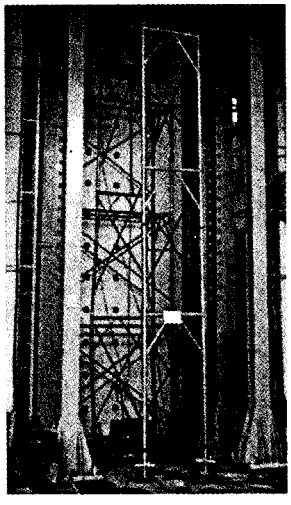

(c) Two-set, three-story tests

Fig. 13 Experiments for two-set scaffold-shoring systems

(1) Two-set one-story tests (Fig. 13a)
(2) Two-set two-story tests (Fig. 13b)
(3) Two-set three-story tests (Fig. 13c)

These test configurations are shown in Figs. 13(a)-(c), and were used to verify and calibrate the computational results.

Preliminary tests were conducted prior to any of the complete full-scale tests in order to evaluate the overall mechanical behavior and approximate maximum loads. Two sets of linear variable differential transformers (LVDT's) and four sets of strain gauges were installed at the likely critical locations to measure values of displacements and strains. The scaffolds were assembled as straight as possible. Vertical load was applied at a rate of 1 mm/min for all tests.

Experimental failure modes are also shown in Figs. 13(a)-(c). The two-set one-story scaffold shore (Fig. 13a) buckled in the out-of plane direction, while the two-story and three-story scaffold shores (Fig. 13b and c) buckled in the in-plane direction, while maximum lateral displacement occurred at the top of the first story. Experimental critical loads are shown in Fig. 14.

Comparisons of the critical loads and failure modes were made between the experimental and computational results. Fig. 14 shows that the experimental critical loads are always slightly lower than the computational values. This occurs because the connection joints between stories are assumed to be rigid in the numerical model; in reality, this is not the case. Fig. 14 also shows that both experimental and computational results exhibit the same decreasing trend in critical load with increases in the number of stories.

Fig. 13 shows that the experimental failure modes are almost identical to the computational results. Both indicate that all failures occur in the in-plane direction, and that the maximum lateral displacement occurs at the top of the lowest story, implying that buckling occurs first in the lowest story.

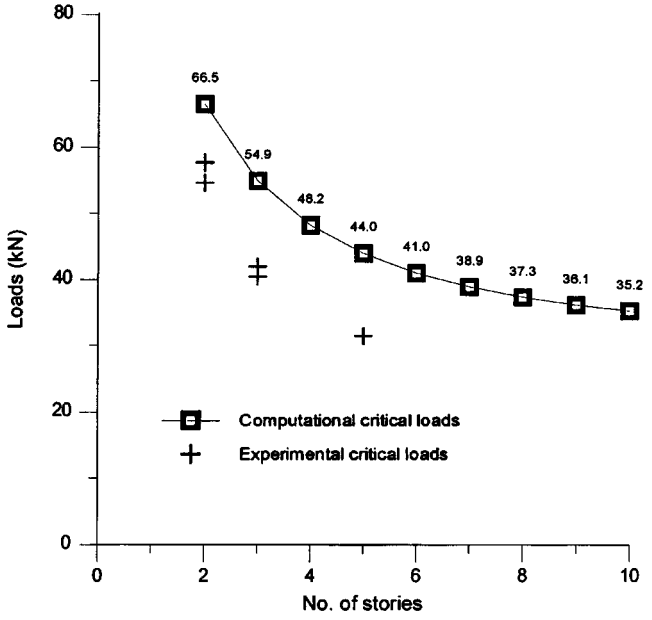

Fig. 14 Computational and experimental critical loads of one-set scaffold-shoring systems

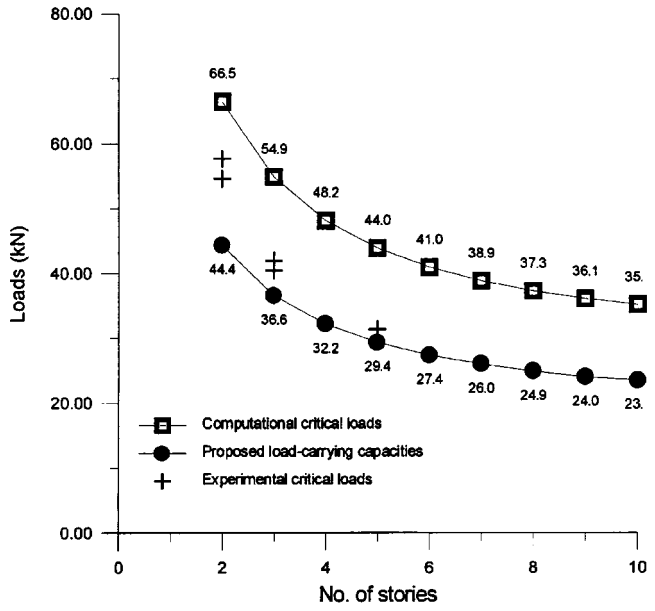

Fig. 15 Computational and experimental critical loads, and proposed design capacities of one-set scaffold-shoring systems

Since the numerical model and full-scale tests indicate the same failure modes and decreasing trend in critical loads, the 2-D model can be regarded as a suitable numerical model for the analysis of typical scaffold shoring systems, even though a small difference was seen between the experimental and computational critical loads. To compensate for this difference, the computational critical loads can be modified for use in design. This modification can be based on the experimental critical loads, and is described in the next section.

5. Load-carrying capacities for scaffold-shoring systems

The reason the computational critical loads are slightly higher than the test results has been previously discussed. In this section, the test results (taken as "actual" values) are used to calibrate the computational results. Since the decreasing trend seen in the computational critical loads is theoretically justified, it is suggested that the magnitudes of load-carrying capacities be based on the test results, while the decreasing trend with increasing number of stories be based on the computational results. Accordingly, the curve describing the relationship between the computational critical loads and the number of stories is then lowered to more closely match the test results. This is accomplished by simply dividing the computational critical loads by a constant number. Theoretically, a fitting point could be determined using a least-square approach. However, in order to be conservative, it is better to simply ensure that all of the experimental critical loads are above the reduced curve (i.e., providing a lower bound curve). A value of 1.5 was found to be the smallest number to achieve this goal. Thus, for practical (design) purposes, a curve reduced by a factor of 1.5 is suggested for use when determining the load-carrying capacity. Fig. 15 shows the computational, experimental and design load-carrying capacities. Note that the design load-carrying

capacity curve exhibits the same decreasing trend as the computational curve, and that all of the experimental critical loads are above this design curve.

As stated previously, if the size of the scaffolds to be used is different from that of the scaffolds considered in this study, the load-carrying capacities should be modified as follows:

$$(P_{cr})_i = P_{cr} \times \frac{E_i I_i / L_i^2}{3830} \tag{1}$$

P_{cr} = values from the modified curve in Fig. 15
$(P_{cr})_i$ = critical loads for scaffold of interest
E_i = Young's modulus for scaffold of interest
I_i = moment of inertia for scaffold of interest
L_i = one-story height for scaffold of interest

For example, if the scaffold of interest has the following properties: E_i=2.05×10^7 N/cm^2, I_i=6 cm^4 and L_i=170 cm^2, the load-carrying capacity of a 7-story scaffold system built with this type of scaffold can be determined as follows:

(1) $\frac{E_i I_i}{L_i^2}$=4256

(2) For 7-story scaffolds, P_{cr} is 26.0 kN from Fig. 15.

(3) The load-carrying capacity for a 7-story scaffold system built with this type of scaffold is therefore

$$P_{cr} = 26.0 \times 4256/3830 = 28.9 \text{ kN}.$$

6. Conclusions

A scaffold-shoring system typically consists of a combination of posts and scaffolds. The connection joints between the scaffolds and posts are generally the critical locations because sidesway can occur there, causing the shoring system to fail. As a result, bracing against sidesway at these locations is very important and should be rigorously checked.

A 2-D model was sequentially derived from consideration of an entire scaffold-shoring system. The 2-D model has the same structural behavior, critical loads and failure modes as the complete scaffold system. The 2-D model is therefore recommended for use as an analysis model for typical scaffold-shoring systems. Using the 2-D model, the critical loads and failure modes can be evaluated relatively quickly using FEA methods.

According to the computational results, the critical loads were found to be related to the factor EI/L^2 of the vertical bars. Therefore, the computational critical loads in this study can be modified for different size scaffolds using a simple factor $(E_i I_i/L^2)/3830$.

In the comparisons of computational and experimental critical loads, the experimental values are slightly smaller than the computational values; however, both exhibit similar decreasing trends with an increasing number of stories. In the comparisons of the failure modes, both computational and experimental results exhibit the same patterns. Thus, the 2-D model is found to be a simple and suitable numerical model for analytical purposes.

It is recommended that the magnitudes of proposed design capacities be based on the

experimental results, and that the decreasing trend with increasing number of stories be based on the computational results. To this end, a design capacity curve was derived by dividing the computational critical loads by a constant 1.5. Finally, it is proposed that the design capacities for different size scaffold-shoring systems be obtained by multiplying the design capacities from this curve by a factor of $(E_i I_i / L^2)/3830$.

Acknowledgements

This study was conducted by the authors under the sponsorship of the Council of Labor Affairs, Taiwan, ROC.

References

Ayyub, B.M. and Eldukair, Z.A. (1989), "Impact of errors on safety during construction", *Proceedings of the Sessions Related to Design, Analysis and Testing, ASCE Structures Congress,* San Francisco, May.

Jan, T.S. (1987), "General instability of scaffold", *Proceedings of International Conference on Structural Failure,* Singapore.

Kao, C.C. (1981), "Analysis of safety behavior for steel scaffold and vertical shore", Report, Department of Civil Engineering, National Taiwan University, Taiwan.

Matousek, M. and Schneider (1977), "Untersuchungen zur struktur des seicherheits problems bei bauwerken", Report No. 59, Institute of Structural Engineering, Swiss Federal Institute of Technology, Zurich.

Peng, J.L., Pan, A.D., Rosowsky, D.V., Chen, W.F., Yen, T. and Chan, S.L. (1996), "High clearance scaffold systems during construction, I: Structural modeling and modes of failure", *Engineering Structures*, **18**(3), 247-257.

Yen, T., Chen, W.F., Lin, C.H., Go, C.G., Ju, M.S., Huang, Y.L., Chen, H.J., Rosowsky, D.V. and Pan, A.D. (1993), "Research of steel scaffold accident during construction period", Labor Checking Report, the Council of Labor Affairs, Taipei, Taiwan, 156.

Yen, T., Chen, W.F., Lin, Y.C., Huang, Y.L. and Chen, H.J. (1994), "Study of steel scaffold supports subjected to unsymmetrical loads and lateral loads", Labor Checking Report IOSH 83-S222, the Council of Labor Affairs, Taipei, Taiwan, 197.

Yen, T., Chen, W.F., Lin, Y.C., Huang, Y.L. and Chen, H.J. (1995), "Study of the interaction between wooden shores and steel scaffolds and development of collapse warning system", Labor Checking Report IOSH 84-S121, the Council of Labor Affairs, Taipei, Taiwan, 95.

Yen, T, Chen, H.J., Huang, Y.L., Chen, W.F., Chi, R.C. and Lin, Y.C. (1997), "Design of scaffold shores for concrete buildings during construction", *Journal of the Chinese Institute of Engineers,* **20**(6), 603-614.

Walker, A.C. (1981), "Study and analysis of the first 120 failure cases", Report: Structural Failures in Buildings, The Institution of Structural Engineers, London.